Quaternaire
Revue de l'Association française pour l'étude du Quaternaire

vol. 22/1 | 2011
Volume 22 Numéro 1

Composition of tephra of the Goldberg volcano (West Eifel, Germany) and search for itS dispersion

Composition du tephra du volcan Goldberg (Eifel occidental, Allemagne) et recherche de sa dispersion

Sébastien Cools, Etienne Juvigné and André Pouclet

Electronic version
URL: http://journals.openedition.org/quaternaire/5834
DOI: 10.4000/quaternaire.5834
ISSN: 1965-0795

Publisher
Association française pour l'étude du quaternaire

Printed version
Date of publication: 1 March 2011
Number of pages: 47-60
ISSN: 1142-2904

Electronic reference
Sébastien Cools, Etienne Juvigné and André Pouclet, « Composition of tephra of the Goldberg volcano (West Eifel, Germany) and search for itS dispersion », *Quaternaire* [Online], vol. 22/1 | 2011, Online since 01 March 2014, connection on 20 April 2019. URL : http://journals.openedition.org/quaternaire/5834 ; DOI : 10.4000/quaternaire.5834

Quaternaire, **22**, (1), *2011*, p. 47-60

COMPOSITION OF TEPHRA OF THE GOLDBERG VOLCANO (WEST EIFEL, GERMANY) AND SEARCH FOR ITS DISPERSION

Sébastien COOLS [1], Étienne JUVIGNÉ [1] & André POUCLET [2]

ABSTRACT

Because of intensive exploitation of the Goldberg volcano (West Eifel Volcanic Field, Germany), in the past three decades, additional information has been obtained on its volcanological history and its products. Two important explosive events are recorded in the stratigraphic pile. An attempt is made to trace tephra of the volcano, by sampling soils in plateau position all around the volcano. However, the sampled sites also contained minerals from the Laacher See tephra that blanketed the area as demonstrated by the occurrence of a layer in the nearby Bragphenn peat bog. We performed electronic microprobe analyses, to discriminate between the pyroxenes from Goldberg and those from the Laacher See. Since the quantities of minerals drop rapidly away from the volcano, the Goldberg tephra cannot be traced beyond some 6 km. Nevertheless the dispersion is more important in westwards so that further discovery of the tephra can be expected especially in Upper Belgium. Our results allow us to shift the minimal age of the eruption from 11.6 ka BP to 25 ka BP.

Keywords: Germany, Eifel, volcano, Goldberg, Laacher See, tephra, geomorphology, Upper- and Middle Pleistocene.

RÉSUMÉ

COMPOSITION DU TÉPHRA DU VOLCAN GOLDBERG (EIFEL OCCIDENTAL, ALLEMAGNE) ET RECHERCHE DE SA DISPERSION

En profitant de l'exploitation intensive du volcan Goldberg (Eifel occidental, Allemagne) au cours des trois dernières décennies, des informations nouvelles sont apportées concernant l'histoire volcanique de l'appareil et de ses produits. Deux importantes phases explosives sont attestées dans sa lithostratigraphie. En l'absence d'affleurements de téphra en place en dehors du volcan, la recherche des lobes est abordée par l'étude des concentrations de minéraux dans des sols actuels en position de plateau. Toutefois les sites étudiés contiennent également des produits du volcan du Laacher See qui sont retombés sur l'Eifel et l'Ardenne (Belgique), et dont nous avons découvert une lamine en place dans une tourbière locale (Bragphenn). En raison du mélange des téphras dans les échantillons de sols actuels, des analyses ont été réalisées au moyen de la microsonde électronique pour distinguer les pyroxènes du téphra du Goldberg de ceux du Laacher See. La méthode n'a pas permis de suivre le téphra à plus de 6 km du volcan, car la concentration de ses minéraux est trop faible au-delà. Néanmoins la dispersion étant plus importante vers l'ouest, c'est donc en haute Belgique que des découvertes ultérieures de ce téphra sont attendues. Nos résultats permettent de vieillir l'âge minimal de l'éruption de 11,6 ka BP à 25 ka BP.

Mots-clés : Allemagne, Eifel, volcan, Goldberg, Laacher See, téphra, géomorphologie, Pléistocène moyen et récent.

1 - INTRODUCTION

The Goldberg is one of the 250 volcanoes of the West Eifel Volcanic Field (WEVF) (fig. 1). The age of most of those volcanoes is currently unknown within the main eruptive epoch in the relevant field that has lasted mainly throughout the Middle and the Late Pleistocene (Büchel & Lorenz, 1982; Mertes & Schmincke, 1983). Since the Goldberg is located in Germany, 4 km beyond the Belgian boundary (fig. 1), the presence of its tephra could be suspected at least in the eastern part of Belgium. The aim of this study is to specify the volcanic style eruption of this volcano and to point out the tephra and mineral composition. Then, extensive sampling of soils is carried out all around the volcano, to search for its tephra dispersion, with the hope to add a new marker in the Pleistocene tephrostratigraphical model of West Germany and East Belgium.

In Belgium, four tephra markers are known in the Upper Pleistocene terrains. They are below from the youngest to the oldest.

– The western lobe of the Upper Laacher See Tephra (ULST) (Juvigné, 1977a; van den Bogaard & Schmincke, 1985) is characterized by phonolitic glass (van den Bogaard & Schmincke, 1985) and titanite as indicator mineral (Juvigné, 1977a, 1993). It originated from the Laacher See volcano of the East Eifel Volcanic Field (EEVF) some 13,000 years ago according to the following

[1] *University of Liège*, Laboratory of Geomorphology and Quaternary Geology, Sart Tilman, 12A, B-4000 LIÈGE.
Courriel: ejuvigne@skynet.be
[2] *University of Orléans* and 1383 rue de la Source, F-45160 OLIVET

Manuscrit reçu le 01/02/2010, accepté le 30/09/2010

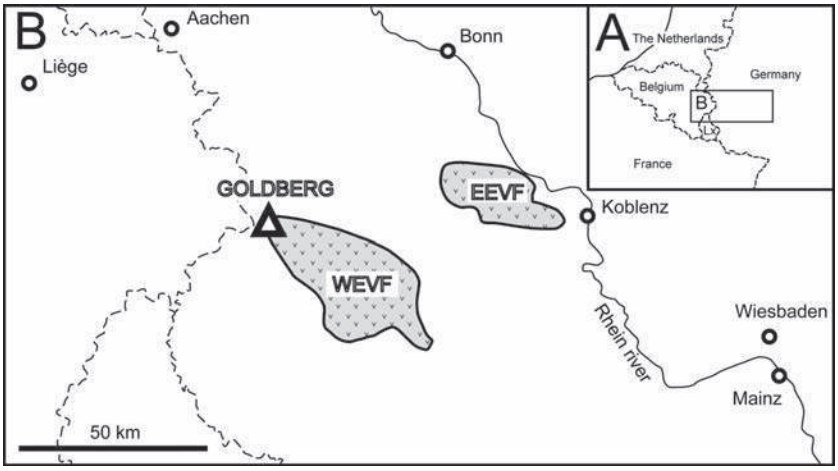

Fig. 1: Location of the Goldberg volcano, as well as the West and East Eifel volcanic fields respectively.
Fig. 1 : Localisation du volcan Goldberg, ainsi que des champs volcaniques respectifs de l'Eifel occidental et de l'Eifel oriental.

selected data: van den Bogaard (1995): 12,900 ± 1120 BP, Ar^{39}/Ar^{40}; Brauer *et al.* (1998a, b): 12,880 ± 120 BP, varve years; Reimer *et al.* (2004): 13,060-12,910, cal ^{14}C age of numerous tree remnants buried by the LST; Blockey *et al.* (2008): 12,975-12,743 cal BP, lacustrine sequence.

– The Eltville Tephra (Rohdenburg & Semmel, 1971; Juvigné & Semmel, 1981) has olivine as indicator mineral. It is dated at about 20 ka and despite the fact that the relevant volcano is not precisely known, it should be in the EEVF (Pouclet & Juvigné, 2009). The glass material is altered into illite, thus its initial chemical composition is unknown. However, the mineral composition belongs to a basaltic alkaline magma compatible with an Eifel volcanic origin.

– The Rocourt Tephra (Gullentops, 1954; Juvigné, 1977b) dated between 74 and 90 ka displays altered blocky shards and a distinct mineralogical association characterized by the occurrence of enstatite (Pouclet *et al*., 2008). The geographical grain-size distribution and the chemical composition of the minerals indicate an origin from the West Eifel Volcanic Field (WEVF).

– The Remouchamps Tephra present in two Belgian caves is dated between 90 ka and 112 ka (Gewelt & Juvigné, 1986; Pouclet *et al*., 2008). It is limited to volcanic fragments preserved in speleothems. The rhyolitic composition of the glass and the mineral assemblage of ferri-tschermakite and hypersthene indicate an evolved tholeiitic magmatic signature, and a possible origin from Iceland, owing to its resemblance to Late Quaternary Iceland ash deposits in northern Europe (Davies *et al*., 2005).

The assumption for additional tephra markers in West Germany and Belgium is a pending question. Bustamante Santa Cruz (1974) pointed out the presence of euhedral to subhedral clinopyroxenes, both in the flood plain of the Amblève river (Belgium) and in the Goldberg volcano. The author concluded that the Goldberg tephra is present in the Amblève valley. Nevertheless, due to the presence of clinopyroxenes in other tephras from the Eifel Fields (ULST, Eltville and Rocourt) in Belgium, the argument of Bustamante Santa Cruz (1974) has become weak.

The study of the Goldberg by Rahm (1961) and Mertes (1983) does not provide sufficient mineralogical and geochemical data to identify distal occurrences of its tephra. Moreover the pyroclasts of the Goldberg have to be distinguished from Upper Laacher See Tephra (ULST), which is present everywhere in the studied area. Other tephras have also blanketed the area: Eltville Tephra and Rocourt Tephra. Hence, hereafter, we investigated in details, both the pyroclasts of the Goldberg and the volcanic materials in the surrounding of the volcano.

2 - THE GOLDBERG VOLCANO

The Goldberg volcano has formed throughout a plateau constituted by Early Devonian slates and sandstones (fig. 2). The local structural pattern shows two fault systems. The SW-NE fractures date back to the Variscan

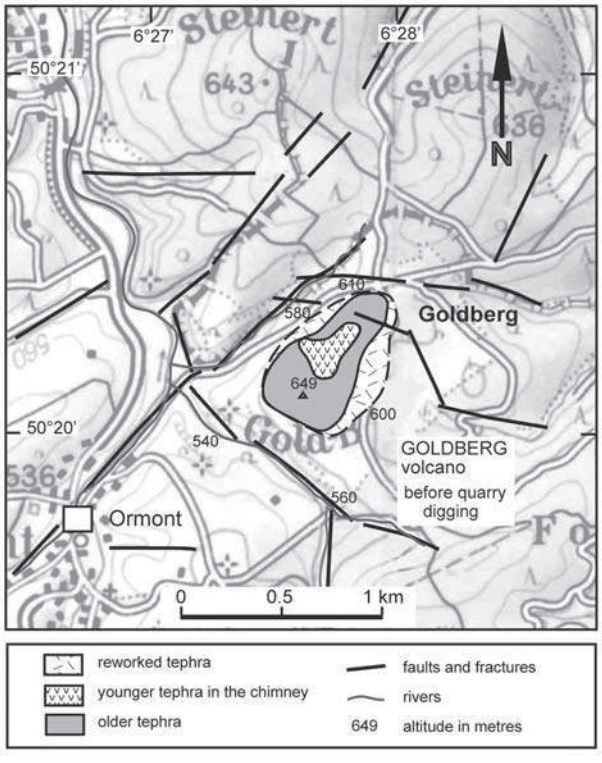

Fig. 2: The Goldberg volcano and the regional structural features.
Fig. 2 : Le volcan Goldberg dans le cadre structural regional.

orogeny. The SE-NW to ESE-WNW faults are related to the recent Rhine Graben tectonic formation. The Goldberg volcano is controlled by this latter fault set.

Present-day, the volcano is severely destroyed by the quarry digging. After Rahm (1961), it was constituted by two neighbouring hillocks aligned NE-SW. These mounds are remnants of a former edifice made up of older tephra. The crater area is defined by younger tephra localized in saddle between the two hillocks. Mertes (1983) provided the stratigraphy of the Goldberg volcano as well as one chemical analysis. Cools (2004) described the spreading of volcanic minerals in the surroundings.

2.1 - VOLCANOLOGICAL FEATURES

For Mertes (1983), the Goldberg is a scoria cone of which accumulation of products is divided in three phases separated by two unconformities. Thanks to the progress of the quarry digging, additional investigations have been conducted to document the volcanological story of the Goldberg before its forthcoming disappearance (fig. 3).

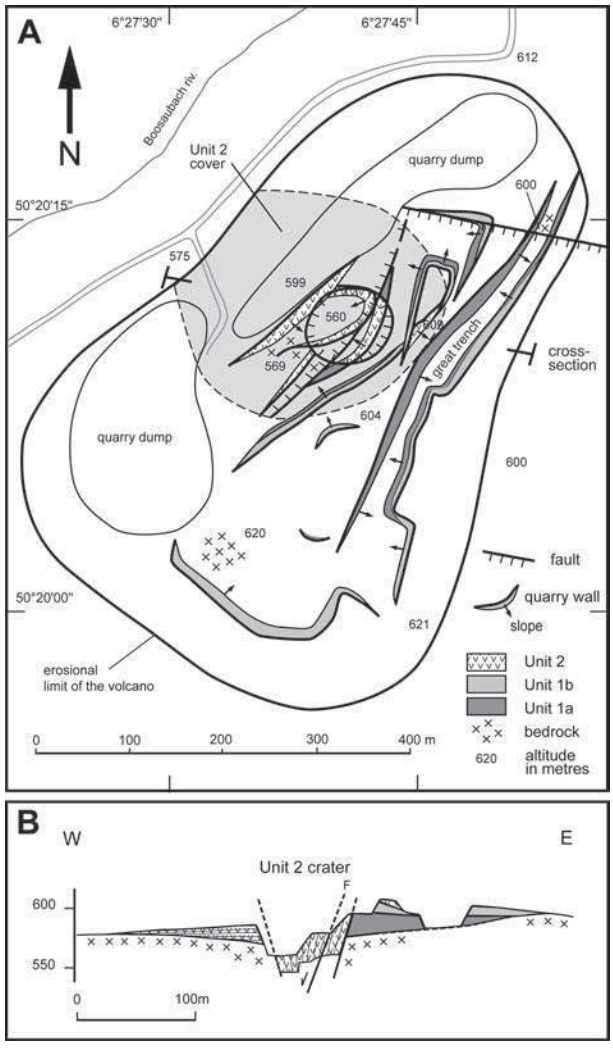

Fig. 3: Mapping of the Goldberg quarry in 2009.
A) Distinction of the volcaniclastic units along the quarry walls and interpretation of the Unit 2 crater area. B) West-East cross-section right on the crater area.
Fig. 3 : Cartographie de la carrière du Goldberg en 2009. A) Distinction des unités volcanoclastiques le long des fronts de taille et interprétation de l'Unité 2 de la zone du cratère. B) Coupe W-E passant par l'aire cratérale.

First, we observed that the setting of all the volcanic products is compatible with a single origin from the same crater area. The present day SSW-NNE elongated shape of the volcano may have resulted from erosional removal of the northwestern flank by the neighbouring brook. No fissural features are preserved in the crater area. But, a NNE-SSW normal fault cuts the crater, with a westward collapse. Moreover, a N.100 -trending normal fault cut the northeastern part of the volcano with a 2 m vertical motion corresponding to uplift of the northern side and lowering of the southern side (Plate 1, photo A). This tectonic event occurred during the last stage of the volcanic activity, because the upper volcaniclastic deposits are only partly affected by the displacement. It is related to the collapse of the inner part of the volcano. Such faulting may be linked to the Rhine Graben tectonic system (fig. 2). The quarry has reached the Devonian basement in many parts, at different altitudes: 620 m at the southern hillock, which was cover by 29 m of volcanic products, 600 m at the northern hillock, and 569 m at the crater edge (fig. 3). The crater area has collapsed, because the basement level is at 575 m to the west of the volcano and at 600 m to the east.

Two different groups of volcanic materials are distinguished, Unit 1 and Unit 2, which belong to two successive phreatomagmatic and strombolian phases. The first group, Unit 1, belongs to the initial edifice. It consists of pyroclastic and basement debris fall and flows. The activity began with the formation of a xenolith-rich and poorly bedded breccia deposit that rests above a palaeosol. This deposit reaches the thickness of 2 m at the crater edge (Plate 1, photo B). It obviously resulted from an initial phreatomagmatic and diatreme-like explosion. Then, the area was covered by gently dipping volcaniclastic deposits by a combination of pyroclastic fall and flows. Some intercalated lithic-rich beds revealed the intermittency of explosive phreatomagmatic pulses. Particularly, the middle level of the pile includes a metre-thick bed of a fallout lithic-rich breccia that can be seen almost continuously from the south and east of the crater to the northeastern margin of the volcano. In addition, the southeastern part of the volcanic pile shows an angular unconformity due to the scraping of the flank beds and to the flowing of a major surge (Plate 1, photo C). The intercalated thick breccia and the great surge associated with the downfall of the southeastern flank indicate an explosive event, with enlargement of the crater, blasting of the southeastern and southern part of the previous edifice, and vertical motion along the N.100 fault. This event and its volcano-tectonic consequences allow us to distinguish two stages in the phreatomagmatic phase of the volcanological story. The first stage corresponds to the crater opening and to the deposition of the lithological Unit 1a in the whole volcano area. The second stage is characterized by the deposition of the lithological Unit 1b beginning with a thick breccia and an unconformable overlapping surge.

The second group of volcanic materials, Unit 2, is located in and around the crater, and corresponds to the younger tephra of Rahm (1961) (fig. 2). It consists of

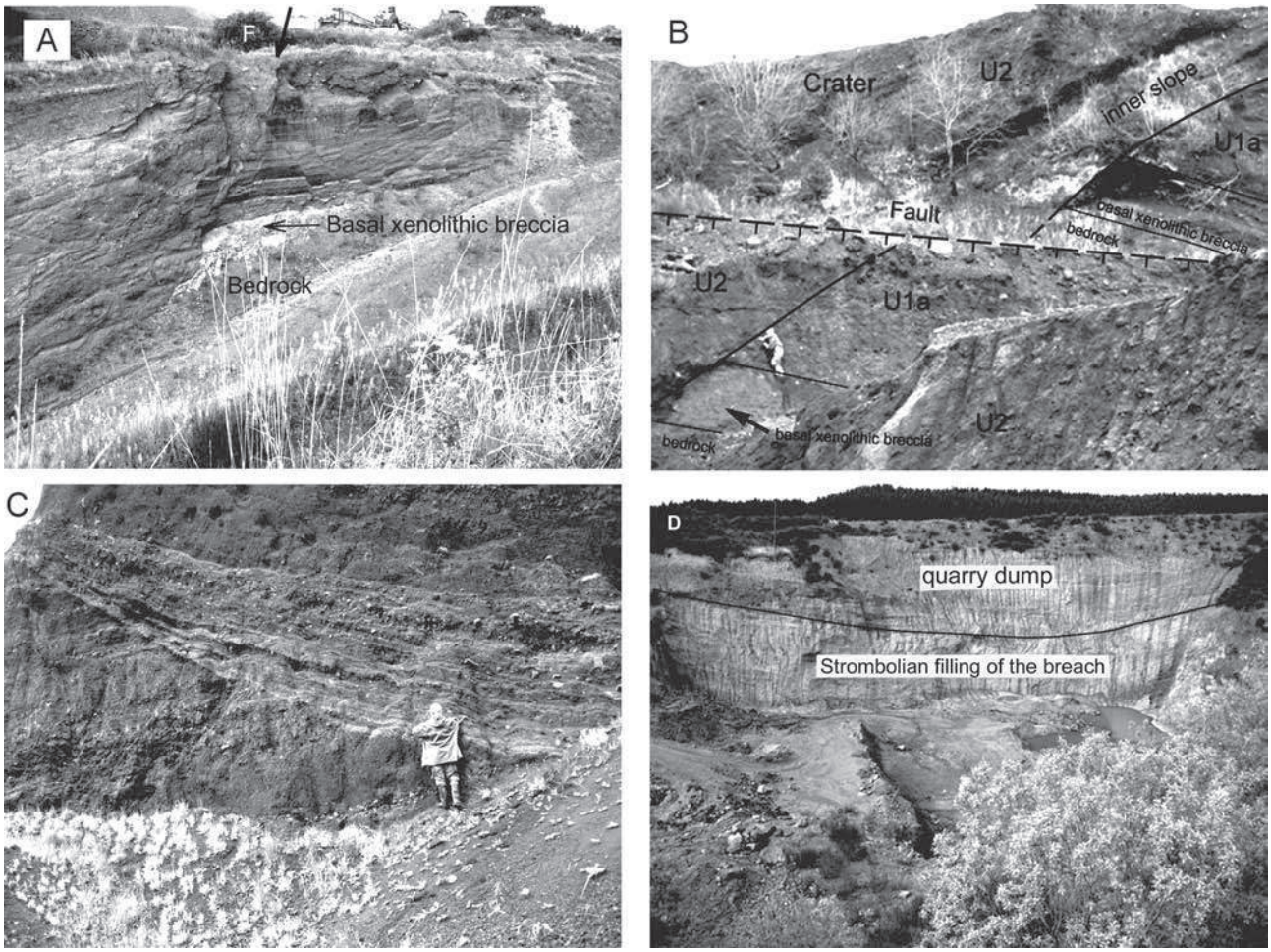

Plate 1:
Photo A: N.100 -trending normal fault cutting the northeastern part of the volcano with a 2 m vertical motion corresponding to uplift of the northern side and lowering of the southern side.
Photo B: Inner slope of the strombolian crater showing the 50° -dipping welded scoria layers and spatter flows (Unit 2) above the phreatomagmatic formations (Unit 1) that began with the xenolith rich breccia.
Vertical displacement of the Unit 1 deposits and of the basement resulted from the NNE-SSW fault motion.
Photo C: Angular unconformity between the Units 1a and 1b due to the scrapping of the flank of the initial cone and to the flowing of a major surge that resulted from a violent explosive event.
Photo D: Filling up of the western saddle of the strombolian crater by the late Unit 2 deposits.
Note overlying quarry dump above black line.
Planche 1 :
Photo A : Faille normale de direction N.100 recoupant la partie nord-est du volcan avec un mouvement vertical de 2 m correspondant au soulèvement de la partie septentrionale et à l'abaissement de la partie méridionale.
Photo B : Pente interne du cratère strombolien montrant l'inclinaison à 50° des couches de scories soudées et des lentilles de lave (Unité 2) surmontant des formations phréatomagmatiques (Unité 1) qui commencent avec une brèche riche en xénolithes. Le déplacement vertical des dépôts de l'Unité 1 et du substratum résulte du mouvement de la faille NNE-SSW.
Photo C : Discordance angulaire entre les Unités 1a et 1b, due à l'abrasion des flancs du cône initial et à l'écoulement d'une déferlante majeure résultant d'un événement explosif violent.
Photo D : Colmatage de l'ensellement occidental du cratère strombolien par les dépôts ultimes de l'Unité 2. Noter une couverture de remblais de la carrière au-dessus de la ligne noire.

spatter and cinder formations related to a common lava fountaining. This activity belongs to the strombolian phase of the volcanic evolution, after the cessation of the phreatomagmatic explosive activity. It was initiated by a major volcano-tectonic event with a ten-metre-thick downwarping of the western side of the first edifice along the NNE-SSW fault. The strombolian products took place in the crater, where the 50°-dipping inner walls were made of welded scoriae, blocks, and spatter flows. They deposited on the crater rim, where the welded tuffs overlie the volcaniclastic beds of the Phase 1 activity. To the western side, the crater was widely opened as a consequence of the NNE-SSW faulting and western downward removal of the previous phreatomagmatic deposits. There, the spatter and cinder products blanketed the basement and filled up the opening (Plate 1, photo D). These products are related to the building of a common strombolian cone until the decreasing and the end of the volcanic activity.

The significant result of this volcanological study is that, in spite of its small size, the Goldberg volcano was able to produce tephra some tens of kilometers away because of its, at least, two explosive events. First, the activity started with a violent phreatomagmatic explosion. Then,

a new explosion destroyed a large part of the first edifice, as shown by the deposition of a thick breccia layer and the unconformable overlap of a surge in the southeastern area. Finally, a drastic volcano-tectonic event caused the removal of all the western part of the phreatomagmatic edifice and initiated the strombolian activity.

2.2 - PETROGRAPHICAL OBSERVATIONS

Rahm (1961) identified clinopyroxene as the dominant mafic mineral along with biotite. Bustamante Santa Cruz (1974) performed microprobe analyses of five clinopyroxenes from the Golberg, which were classified as titanoaugite. Mertes (1983) confirmed the prevalence of clinopyroxene over biotite in the Goldberg products. In addition, this author provided one chemical analysis of the lava, which is indicative of a pyroxene- and olivine-rich leucite nephelinite composition, according to the norm calculation.

We investigated lava samples from spatter flows, massive bombs, scoriae and lapillis. Texture is hyalo-microlitic porphyritic and seriate with abundant phenocrysts of pale green clinopyroxene, flakes of phlogopite, and less abundant phenocrysts and microphenocrysts of olivine highly replaced by iddingsite at the border and along the cracks. Large aggregated megacrysts of greenish clinopyroxene are common. The matrix is made of microcrysts of the same minerals plus microlitic melilite, nepheline, deep brown spinel and iron oxides. The glassy groundmass is rich in interstitial nepheline and leucite. One must note the absence of amphibole. The rock is named: pyroxene, phlogopite-, and olivine-phyric leucite melilite nephelinite. The scoriae and lapilli contain numerous fragments of clinopyroxene and flakes of phlogopite, but scarse olivine. It is suggested that explosive processes strongly fragmented the oxidized and fissured crystals of olivine.

Finally, the noteworthy original composition of the Goldberg volcaniclastic products is as follow: abundant clinopyroxene, moderate amount of mica, rare olivine, and absence of amphibole.

3 - ANALYSES OF GOLDBERG PRODUCTS

The study of the Goldberg tephra has been conducted from the volcano to the surrounding area. Special search has been done in a peatbog and in the soils (fig. 4).

3.1 - SAMPLING

Volcano. Ten samples of the pyroclastites were taken in various parts of the volcano throughout the stratigraphical column, in order to detect variations of the lava composition during the volcanic eruption.

Peat bog. The Bragphenn peatbog, 3 km SW of the Goldberg (fig. 4) was investigated. But it is devoid of Goldberg products. We only discovered the Upper Laacher See Tephra (ULST) within the peat.

Surrounding soils. Since no products from the Golberg were observed in roadcuts or trenches in the surroundings of the volcano, 48 samples were taken from present soils on flat surfaces, most of them in plateau position (fig. 4). In such sites, minerals of the ULST are present since the area is part of the western lobe of the Laacher See volcano (Juvigné, 1977a; van den Bogaard & Schmincke, 1985). The main question is whether the Goldberg tephra is also preserved in such sites despite its old age. Of course, tephras from other Eifelian volcanoes could also be present in the area; for instance the region is on the route of the Eltville Tephra and the Rocourt Tephra originating from the Eifel and present in Belgium (Juvigné, 1993). Furthermore, ashes from nearby volcanoes of the WEVF transported by NW winds could also be mixed into the soils.

At all sites, a hole was dug down to the basement with a spade (generally 15 to 20 cm in depth). The present soil is very thin: about 10 cm of loess, with additional humus in forests. It overlies a few centimetres of gravely silt, then the basement. Since the tephra minerals are mixed in the soil, mainly by bioturbation, as it was demonstrated for the ULST minerals (Juvigné, 1977a), a single sample (between 100 to 150 g) was taken, from the surface to the basement.

3.2 - LABORATORY METHODS

Smear slides. In the silt fraction, the tephra material is scarce, because the matrix of the host sediments of present soils is essentially composed of allochtonous loess, and loam from altered Devonian shales and sandstones, rich in heavy minerals. On the contrary, volcanic grains widely dominate in the sandy fraction in which the grain-

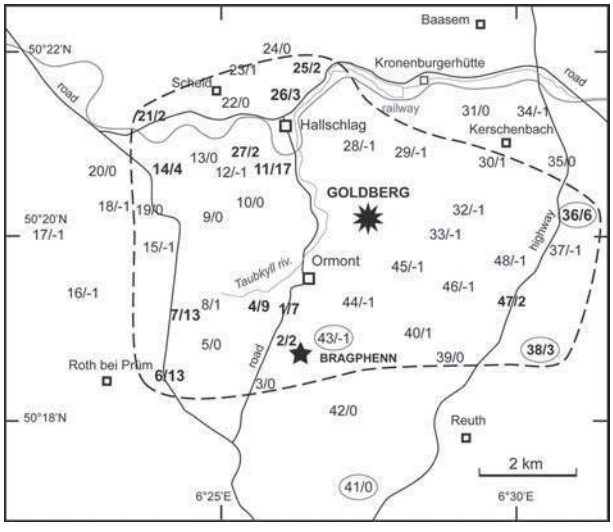

Fig. 4: Sampling sites and excess of clinopyroxene vs titanite in present soil.
On the left side of the slash, numbers localize samples 1 to 48 taken from present soils on flat surfaces in plateau position. On the right side of the slash, excesses of clinopyroxene vs titanite in present soils, in comparaison to the ratio of the heavy mineral suite of the ULST (see tab. 5); higher excesses are in bold. The circled numbers locate the olivine-rich sites. Black star = Goldberg; B = Bragphenn peat bog.
Fig. 4 : Les nombres à gauche du slash correspondent à la numérotation des échantillons 1 à 48 prélevés dans les sols actuels sur des surfaces subhorizontales de plateaux. Les nombres à droite du slash correspondent aux excès de clinopyroxènes/titanite en comparaison avec celui du ULST (voir tab. 5) ; les excédents les plus élevés sont en gras. Les sites encerclés sont ceux qui contiennent de l'olivine. Etoile noire = Goldberg ; B = Tourbière de Bragphenn.

size ranges between 105 and 420 µm. This sandy fraction represents only 3 to 15 % of the bulk samples. The same fraction (105-420 µm) was investigated in each sample, from the volcano itself, the present soil, and the ULST of the Bragphenn peat-bog, in order to facilitate the attempts of correlations. Treatment of each sample was as follows: 1) boiling in H_2O_2, then HCl-10 % to destroy the cements of aggregates; 2) sieving in water current to gather the fraction 105-420 µm; 3) mounting of smear slides of bulk material; 4) extraction of heavy minerals from 1 g of the 105-420 µm fraction by centrifugation in bromoform (density = 2.8).

Microprobe analyses. For the whole-rock chemical analyses, a few tiny scoriae were crushed to powder, of which 20 mg was mixed with the same weight of lithium tetraborate. The mixture was fused into glass that was crushed in fragments.

Smear slides of the heavy minerals, pyroclasts, and vitrified shards were polished for analyses. The analyses were done with a Cameca SX-50 calibrated as follows: 15 kV, 6 to 10 nA, time count of 6 (Na, K), 10 (Fe, Mn, Cr), 12 (Ca, Ti), and 16 seconds (Si, Al, Mg). We only analyzed the mafic minerals. Feldspars are present, but they cannot be used for the tephra discrimination in the loess deposits, because it is impossible to determine if they belong to the tephra or to detritical sediments.

4 - PYROCLASTITES OF THE GOLDBERG TEPHRA

4.1 - MAFIC MINERALS

The samples contain about 95 % of pyroclasts and 5 % of crystals with some mesostase coating. In all smear slides of heavy material, the clinopyroxenes widely dominate; they exhibit three facies in almost equal parts: euhedral crystals, broken fragments of euhedral crystals, and shards from broken megacrysts. Brown micas are also common minerals in smear slides. A few olivine crystals are present in one sample from a scoria layer of Unit 1b in the southern most part of the quarry, some 8 m below the present soil. Microprobe analyses of minerals were performed on three samples from Goldberg volcano (tab. 1A, 1B and 1C). The compositions of pyroxenes and olivines are represented in figure 5.

The minerals are described hereafter in their abundance order.

The clinopyroxenes consist in fassaitic diopside along with a minority of diopside (tab. 1A, fig. 5), with the range composition of $47.3 < XMg\ \% < 37.6$, $7.4 < XFe^{2+} + Mn\ \% < 2.4$, $58.0 < XCa\ \% < 48.0$ (table 1A). As for many pyroxenes from alkaline lavas, they widely overlap the 50 % Ca limit, and plot in the fassaitic area. This is due to their high Al and Ti contents, and so, their high amount of Ca- and Ti-tschermakite end-members. Besides, their Na-content is low.

The brown micas are highly magnesian ($0.79 < Mg/Mg+Fe^{2+} < 0.85$) (tab. 1B). They consist in phlogopite, according to the phlogopite-biotite division, where Mg:Fe = 2:1. They are titanian-rich ($3.9 < TiO_2$ weight $\% < 4.7$), a common feature of micas from alkaline rocks.

The olivines display a Fo-content of 85.6 to 87.1 (tab. 1C; fig. 5B), a common composition for olivines from alkaline mafic lavas.

4.2 - COMPOSITION OF THE PYROCLASTS OF THE CONE

We analysed ten samples of pyroclasts of the cones, from the basal deposit of Unit 1 to the upper agglutinates of Unit 2 in the crater. For each sample, four analyses were carried out. The results are given in table 2. Totals of oxides average 50 % due to the tetraborate part. They are corrected to 100 %. All the analyses are quite similar, except for the alkalies that are very low in three samples. These apparent depletions are due to the high heterogeneity of the volcaniclastic material and to the alteration of mobile elements (Na, K). Notwithstanding these anomalies, it can be concluded that there was no significant chemical variation of the lava during the

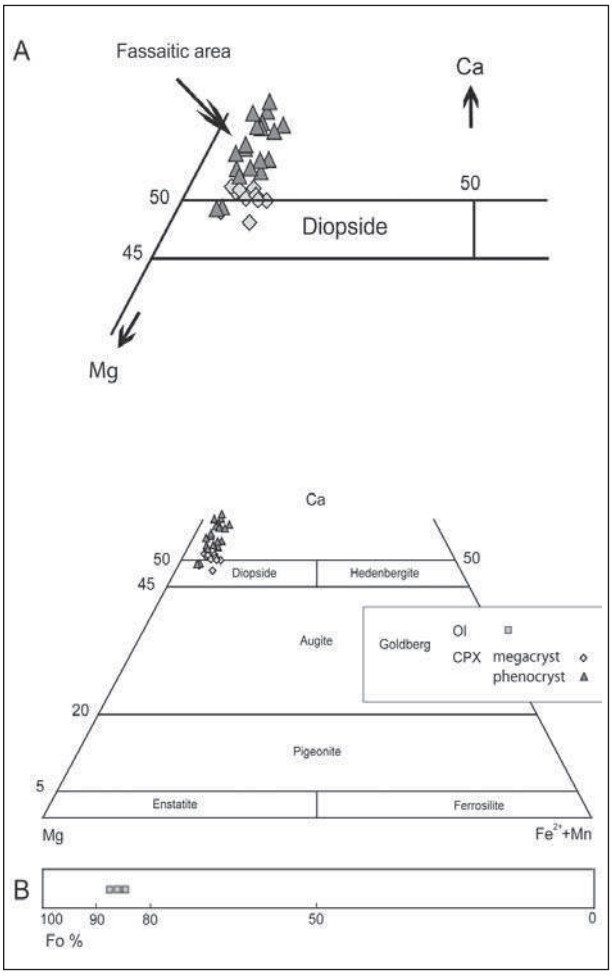

Fig. 5: Determination of mafic minerals from the Goldberg volcano: A) clinopyroxenes (see tab. 1A) after Morimoto's classification (1998). B) olivine (see tab. 1B).
Fig. 5 : Détermination des minéraux mafiques du volcan Goldberg: A) clinopyroxènes (voir tab. 1A) d'après la nomenclature de Morimoto (1998). B) olivine (voir tab. 1B).

	Initial stage phenocrysts			Unit 1 phenocrysts				Unit 1 megacrysts		
SiO_2	41.78	49.08	50.76	43.24	43.97	45.52	45.68	47.70	51.35	51.84
TiO_2	4.61	1.23	0.90	3.17	3.65	2.25	2.75	2.29	1.03	1.08
Al_2O_3	8.91	4.67	4.34	7.52	7.77	7.48	5.38	5.03	4.19	4.43
FeO	7.51	5.71	4.08	7.20	6.67	8.63	6.82	6.08	4.73	5.24
MnO	0.04	0.17	0.06	0.11	0.00	0.00	0.00	0.00	0.12	0.10
MgO	11.45	14.14	15.63	11.85	12.30	11.07	13.11	14.08	15.85	14.52
CaO	23.92	23.70	22.65	23.63	24.02	23.08	23.87	24.47	22.98	23.63
Na_2O	0.29	0.48	0.55	0.25	0.26	0.86	0.29	0.24	0.48	0.50
K_2O	0.00	0.02	0.02	0.06	0.00	0.00	0.05	0.00	0.01	0.00
Cr_2O_3	0.12	0.07	0.58	0.09	0.00	0.00	0.08	0.00	0.01	0.00
Total	98.63	99.27	99.57	97.12	98.64	98.89	98.03	99.89	100.75	101.34
Si	1.585	1.819	1.861	1.659	1.659	1.716	1.731	1.765	1.862	1.880
Ti	0.132	0.034	0.025	0.092	0.104	0.064	0.078	0.064	0.028	0.030
Al	0.399	0.204	0.188	0.340	0.346	0.332	0.240	0.219	0.179	0.190
Fe^{3+}	0.183	0.122	0.064	0.174	0.147	0.170	0.161	0.139	0.075	0.026
Fe^{2+}	0.055	0.055	0.061	0.058	0.063	0.102	0.055	0.049	0.069	0.133
Cr	0.004	0.002	0.017	0.003	0.000	0.000	0.002	0.000	0.000	0.000
Mn	0.001	0.005	0.002	0.004	0.000	0.000	0.000	0.000	0.004	0.003
Mg	0.648	0.781	0.854	0.678	0.692	0.622	0.741	0.777	0.857	0.785
Ca	0.972	0.941	0.889	0.972	0.971	0.932	0.969	0.970	0.893	0.918
Na	0.022	0.035	0.039	0.018	0.019	0.063	0.021	0.017	0.033	0.035
K	0.000	0.001	0.001	0.003	0.000	0.000	0.002	0.000	0.001	0.000
Total	4.001	3.999	4.001	4.001	4.001	4.001	4.000	4.000	4.001	4.000
$100Mg/(Mg+Fe^{2+})$	92.16	93.40	93.32	92.17	91.59	85.89	93.11	94.05	92.59	85.54
Mg %	38.63	43.82	47.28	39.62	40.07	37.56	41.97	43.25	47.03	42.69
Fe" + Mn %	3.37	3.39	3.48	3.58	3.68	6.17	3.11	2.73	3.97	7.38
Ca %	58.00	52.79	49.24	56.79	56.25	56.28	54.92	54.02	49.00	49.93
End-members										
En %	32.42	39.13	43.09	33.99	34.58	31.08	37.10	38.82	42.86	39.26
Fs %	2.83	3.03	3.17	3.07	3.17	5.11	2.75	2.46	3.62	6.79
Wo %	34.80	39.88	39.91	36.34	36.74	35.65	39.06	40.00	39.15	41.41
Ac %	2.16	3.48	3.92	1.85	1.90	6.28	2.11	1.72	3.35	2.61
Jd %	0.00	0.00	0.00	0.00	0.00	0.00	0.00	0.00	0.00	0.92
Ca-Tsch %	0.00	2.34	4.88	0.01	0.46	4.80	0.00	0.00	4.08	6.06
Ti-Tsch %	11.59	3.42	2.50	9.18	10.36	6.38	4.92	4.82	2.80	2.95
Es %	16.20	8.72	2.53	15.56	12.79	10.70	14.06	12.18	4.14	0.00
Ko%	0.00	0.00	0.00	0.00	0.00	0.00	0.00	0.00	0.00	0.00
Total	100.00	100.00	100.00	100.00	100.00	100.00	100.00	100.00	100.00	100.00

Tab. 1A: Chemical composition of representative clinopyroxenes of the Goldberg volcano.
Table of detailed analyses (n=29) can be obtained on request.
Tab. 1A : Composition chimique de clinopyroxènes représentatifs du volcan Goldberg. Le tableau des analyses détaillées (n=29) peut être obtenu sur demande.

SiO_2	36.95	36.98	36.49	36.62	36.80	37.21
TiO_2	3.98	4.18	3.87	3.90	4.30	4.68
Al_2O_3	15.94	15.55	15.71	15.80	15.80	15.24
FeO	8.65	8.09	8.91	8.85	8.83	6.38
MgO	18.37	18.78	18.33	18.60	18.44	19.65
CaO	0.05	0.10	0.08	0.09	0.05	0.08
Na_2O	0.54	0.52	0.53	0.56	0.59	0.33
K_2O	9.90	9.82	9.67	9.83	9.87	10.18
Total	94.38	94.02	93.59	94.25	94.68	93.75
Si	2.717	2.723	2.710	2.702	2.702	2.730
Al	1.382	1.350	1.375	1.374	1.367	1.318
Ti	0.220	0.231	0.216	0.216	0.237	0.258
Fe	0.532	0.498	0.553	0.546	0.542	0.391
Mg	2.014	2.061	2.029	2.046	2.018	2.149
Ca	0.004	0.008	0.006	0.007	0.004	0.006
Na	0.077	0.074	0.076	0.080	0.084	0.047
K	0.931	0.924	0.918	0.927	0.927	0.955
Total	7.876	7.870	7.884	7.898	7.882	7.854
$Mg/Mg+Fe^{2+}$	0.79	0.81	0.79	0.79	0.79	0.85

Tab. 1B: Chemical composition of micas of the Goldberg volcano.
Tab. 1B : Composition chimique des micas du volcan Goldberg.

SiO_2	41.30	40.78	39.95	40.17
TiO_2	0.10	0.03	0.06	0.00
Al_2O_3	0.06	0.10	0.02	0.06
FeO	11.65	11.93	12.33	12.97
MnO	0.20	0.18	0.26	0.33
MgO	44.71	43.81	46.24	44.20
CaO	0.42	0.54	0.62	0.73
Total	98.42	97.38	99.48	98.48
Si	1.034	1.034	0.998	1.015
Ti	0.002	0.001	0.001	0.000
Al	0.002	0.003	0.001	0.002
Fe^{2+}	0.244	0.253	0.258	0.274
Mn	0.004	0.004	0.006	0.007
Mg	1.668	1.655	1.722	1.665
Ca	0.011	0.015	0.017	0.020
Total	2.960	2.960	2.995	2.977
Fo%	87.06	86.57	86.74	85.55

Tab. 1C: Chemical composition of olivines of the Goldberg volcano.
Tab. 1C : Composition chimique des olivines du volcan Goldberg.

	Unit 1							Unit 2				Lava
Sample #	2a	2c	3a	3b	3c	4a	4b	4c	1b	1c	Mean	St Dv	
Nb. of analyses	4	4	4	4	4	4	4	4	4	4			1
SiO_2	42.84	44.35	47.10	44.70	45.37	46.00	46.15	47.11	47.30	44.42	45.53	1.46	42.65
TiO_2	3.54	3.31	2.97	3.15	3.34	3.17	3.48	3.60	3.19	3.22	3.30	0.20	2.94
Al_2O_3	12.20	11.62	11.26	12.05	12.49	12.05	12.40	13.34	11.88	12.13	12.14	0.55	11.67
FeO_t	10.79	9.97	10.21	10.37	9.88	10.75	11.63	12.20	9.82	10.67	10.63	0.77	10.51
MgO	12.72	10.30	9.83	10.77	9.56	9.94	11.30	11.47	9.05	9.56	10.45	1.12	11.56
CaO	16.60	15.56	13.97	14.93	14.94	13.26	13.30	11.50	15.12	15.93	14.51	1.51	15.38
Na_2O	0.50	1.92	1.34	1.24	1.56	1.68	0.61	0.23	2.34	1.32	1.27	0.66	2.44
K_2O	0.81	2.97	3.32	2.79	2.86	3.15	1.13	0.55	1.30	2.75	2.16	1.08	2.85
Total	100.00	100.00	100.00	100.00	100.00	100.00	100.00	100.00	100.00	100.00	100.00		100.00

Tab. 2: Chemical composition of the pyroclasts of the cone. Samples are listed in the stratigraphical order, from the base of Unit 1 to Unit 2. Comparison with the lava composition given by Mertes (1983) excluding MnO value.
Tab. 2 : Composition chimique des pyroclastes du cône. Les échantillons sont rangés dans l'ordre stratigraphique, de la base de l'unité 1 à l'unité 2. Comparaison avec l'analyse de la lave de Mertes (1983) excluant le MnO.

eruption. Then, the composition of the analyzed Goldberg lava can be assumed for the pyroclasts of the whole tephra. Compared with the lava analysis given by Mertes (1983) (tab. 2), the pyroclasts are slightly reacher in Si, Ti, and Al, and slightly poorer in Mg, Ca, and alkalies. These differences can be explained by the abundance of pyroxene phenocrysts in the lava, as it is recorded.

Glass fragments have been selected from pyroclastites of the lower part of Unit 1. As a whole, the glass material is altered, but it is possible to analyze some preserved parts (tab. 3). The seven analyses display some variable amounts of Al_2O_3 (12.7 – 14.7 weight %), MgO (4.5 – 6.9 weight %), CaO (11.1 – 16.0 weight %), Na_2O (3.5 – 5.1 weight %) and K_2O (3.4 – 6.7 weight %). The MgO- and CaO-contents are negatively correlated with the alkalies contents. This is explained by variable fractionation of olivines and pyroxenes from the whole lava. Comparing the averaged glass analysis to the averaged Goldberg lava analysis from Mertes (1983), it is calculated that the lava composition results from the addition of 8 % of olivine and 38 % of pyroxenes to the glass composition.

5 - THE BRAGPHENN PEAT BOG

The Bragphenn peat bog is localized 3 km SW of Goldberg (fig. 6). The site is a saddle between the head of the Rupbach and the Prüm valleys. The Rupbach valley is very wide and without stream in this section. The current upper Prüm has likely flown in the Rupbach valley, until it was captured by the former lower Prüm at the place of the saddle. Backwards erosion profile is present in the upper Prüm river bed some 1500 m upwards. Hence, the present abandoned upper Rupbach valley has become a privilege site for accumulation of deposits.

Various sounding were done to localize where the deposit is the thickest. At this site, a core was taken (fig. 6B) composed as follows:

– 0 to 200 cm, pure peat with macroremnants;

– 200 to 240 cm, pure peat with microremnants;

– 240 to 280 cm, pile of fine layers of gleyified clayey silt or humus containing microremnants of plants (gyttja); at depth 275 cm the Upper Laacher See Tephra is present as a 5 mm thick light grey layer;

– 280 to 375 cm, gleyified clayey silt.

Below 375 cm, the material is a very gravely slope deposit with increasing part of blocks downwards, so that

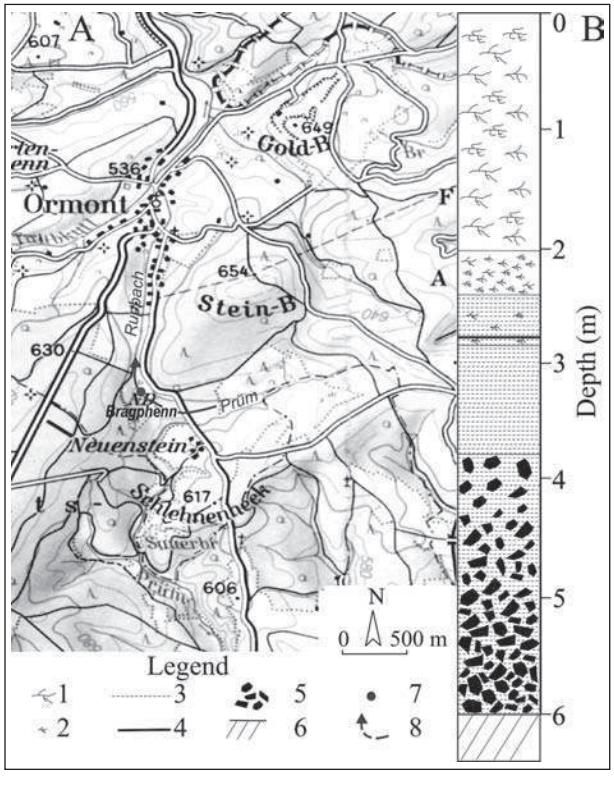

Fig. 6: The Bragphenn site (A) and the lithostratigraphical column at the thickest place of the deposits (B).
Legend: 1, peat with macroremnants; 2, pure fine debris of plants; 3, gleyified clayey silt; 4, Upper Laacher See Tephra; 5, cobbles and blocks; 6, basement; 7, coring site; 8, previous elbow of the upper Prüm river before its capture by the lower Prüm. Background map is from "Topographische Karte 1:100000, C5902, Prüm, Landesvermessungsamt Rheinland-Pfalz".
Fig. 6 : Le site de Bragphenn (A) et la colonne lithostratigraphique à l'endroit où la couverture tourbeuse est la plus épaisse. Légende : 1, tourbe à macrorestes ; 2, petits débris de plantes ; 3, limon argileux gleyifié ; 4, téphra supérieur du Laacher See ; 5, cailloux et blocs ; 6, substratum ; 7, point de carottage : 8, coude de la rivière Prüm avant la capture de sa partie supérieure par la Prüm inférieure. Fond topographique d'après la "Topographische Karte 1:100000, C5902, Prüm, Landesvermessungsamt Rheinland-Pfalz".

Microprobe analyses of the glass pyroclasts									
an. #	23	25	30	31	33	34	37	Mean	St. Dv.
SiO_2	40.78	41.02	40.73	40.71	42.17	41.62	40.27	41.04	0.64
TiO_2	3.19	3.7	3.23	3.03	3.16	3.52	3	3.26	0.26
Al_2O_3	14.42	12.71	13.26	14.24	14.65	13.61	14.43	13.9	0.72
FeO_t	10.28	9.75	10.02	10.29	9.41	10.49	11.11	10.19	0.55
MnO	0.13	0.11	0.25	0.22	0.25	0.2	0.21	0.2	0.05
MgO	4.51	6.85	5.74	4.56	4.98	6.06	4.77	5.35	0.89
CaO	11.05	15.96	12.71	11.17	12.53	12.87	13.49	12.83	1.65
Na_2O	4.83	3.48	4.57	5.13	4.09	3.59	3.66	4.19	0.66
K_2O	6.68	3.43	4.83	6.54	4.39	4.63	4.62	5.02	1.18
Total	95.87	97.01	95.34	95.89	95.63	96.59	95.56	95.98	

Calculated values			
	Averaged glass	54 Glass + 8 Ol + 38 Px	Goldberg lava
SiO_2	42.75	43.72	42.56
TiO_2	3.4	2.99	2.94
Al_2O_3	14.49	10.30	11.65
FeO_t	10.62	9.45	10.49
MnO	0.2	0.15	0.19
MgO	5.58	11.59	11.54
CaO	13.36	16.53	15.36
Na_2O	4.37	2.45	2.43
K_2O	5.23	2.82	2.84
Total	100.00	100.00	100.00

Tab. 3: Electron microprobe analyses of glass pyroclasts and calculated composition of the relevant lava, in adding its phenocrysts, by comparison with the lava composition of Mertes (1983).
Tab. 3 : Analyses par microsonde électronique du verre des pyroclastes et composition chimique calculée de la lave correspondante, en ajoutant ses phénocristaux, par comparaison avec la composition de la lave d'après Mertes (1983)

no core could be taken. The bed-rock was reached at a depth of 6 m.

Since the Laacher See Tephra was found in numerous pollen diagrams in the final phase of the Allerød palynozone and dated at about 13 ka (see above), this tephra provides the opportunity to estimate the age of the over- and underlying terrains. It was demonstrated at numerous sites, in Belgium and in the West Eifel, that the peat cover has formed during the Holocene (e.g. Straka, 1975; Woillard, 1975; Bastin & Juvigné, 1978), so that the peat of the Bragphenn fits with such an age. Hence, the layers of gleyified silt and organic matters interbedded between the ULST and the Holocene peat correspond to the Younger Dryas. Below the ULST, the gleyified loess should correspond to the period of high rate of eolian sedimentation of the Late Weichselian glacial period (Juvigné & Wintle, 1988; Frechen, 1999; Preusser & Frechen, 1999; Frechen *et al*., 2003). This gives an age of about 25 ka to the depth 380 cm of the Bragphenn log. The underlying blocky and gravely body is a solifluxion deposit, likely of Middle Weichselian age. No scoria layer similar to the material of Goldberg was found in the core. It is concluded that the Goldberg is older than the Bragphenn deposits.

6 - PROXIMAL OCCURRENCES OF GOLDBERG TEPHRA

As explained above, the only possibility to look for the Goldberg tephra, apart from the volcano, was to investigate samples taken in present soils in plateau position (fig. 4). Preliminary investigations have shown that neither scoriae nor glass shards are present in the samples, likely due to alteration by pedogenic processes. Hence the search for Goldberg tephra could only be based on heavy minerals, taking into account that the ULST should be present, along with traces of other tephras.

6.1 - HEAVY MINERAL SUITES OF GOLDBERG TEPHRA AND ULST

The heavy mineral suites of samples from the Goldberg volcano and the ULST of the Bragphenn peat bog are represented in table 4.

In the samples from the Goldberg volcano, clino-pyroxene dominates over brown mica. Regarding the percentages, due to free spaces between sheets in

	nb	Clinopyroxene	Brown amphibole	Titanite	Brown mica
GOLDBERG	1520	95	0	0	5
ULST	869	26.4	53.4	20.2	0

Tab. 4: Mafic mineral suites of the Goldberg products and the ULST in the Bragphenn site.
For the Goldberg, percentages were calculated for 1520 minerals distributed in 10 samples taken throughout the stratigraphical series of the volcano. For the ULST, 869 minerals were determined in one slide.
Tab. 4 : Associations de minéraux mafiques des produits du volcan Goldberg et de l'ULST dans le site de Bragphenn. Pour le Goldberg, les pourcentages ont été calculés sur un total de 1520 minéraux distribués dans 10 échantillons de la série stratigraphique du volcan. Pour l'ULST, 869 minéraux ont été déterminés sur un seul frottis.

micas, the density range overlap the bromoform density (d = 2.8), so that micas represents more than 5 % of the suite, and clinopyroxene less than 95 %.

6.2 - MAFIC MINERALS IN PRESENT SOILS ON FLAT SURFACES

A total of 48 samples was taken in present soil on wide flat surfaces (location in figure 4). All sites are within a circle 12 km across around the volcano, where tephra from Goldberg was necessarily deposited at the time of the eruption. Since remnants of that material could be preserved along with tephra from other volcanoes and obviously with the ULST, the aim in this study is to identify the material yielded by the Goldberg volcano. The heavy mineral suites of all samples are presented in table 5.

To distinguish the tephra from Goldberg, we have to take into account the followings, which allow us to detect or to discard the occurrence of other tephra material:

– high amounts of titanite along with brown amphibole in all samples testify that the ULST is present;

– no enstatite was found, so that the presence of material from the Rocourt Tephra and Remouchamps Tephra should be discarded;

– traces of olivine were found, so that the presence of material from the Eltville Tephra cannot be totally excluded, although the olivine may have been provided by any neighbouring volcano, south-east of Goldberg;

– it is not possible to distinguish clinopyroxenes from Goldberg and ULST with an optical microscope alone;

– neither brown amphibole nor titanite are present in the Goldberg products;

– in the products of the West Eifel volcanoes, titanite is rare, while olivine is a common mineral and brown amphibole locally present;

– quantitative variations within the suite of a single tephra were demonstrated for the tephra of the May 18 eruption of Mount St Helens/USA (Juvigné & Shipley, 1983) as a consequence of sorting during transportation of tephra in the stratosphere. So, only the relative abundances have to be considered;

– due to their fragility (cleavages), amphiboles are easily broken while sieving, so that amount of amphiboles is usually overestimated. Therefore, ratio "clinopyroxene/titanite" was only taken into account in the following.

The ratio "clinopyroxene/titanite" was calculated (tab. 5) for the ULST of the Bragphenn peat bog (R = 1.3), and for each sample from present soils. The value 1.3 of ULST was discounted from present soil ratios in order to depict in the latter ones, excesses of clinopyroxenes, which could indicate such minerals yielded by the Goldberg, or may be by other more distal volcanoes. Of course, this assumption does not exclude the presence of clinopyroxenes from Goldberg in samples with ratios lower than 1.3.

Among the 48 investigated soil samples, the excesses (E in the following) of clinopyroxenes can be grouped as follows (tab.5).

	Cpx	Amp	Tit	Oli	Total	Cpx/Tit	(Cpx/Tit) -1.30
ULST	229	464	176	0	869	1.30	
Sample #							
1	390	30	45	0	465	8.67	7.37
2	117	127	37	0	281	3.16	1.86
3	27	83	32	0	142	0.84	-0.46
4	172	75	16	0	263	10.75	9.45
5	53	73	65	0	191	0.82	-0.48
6	154	34	11	0	199	14.00	12.70
7	280	100	20	0	400	14.00	12.70
8	256	218	120	0	594	2.13	0.83
9	50	75	50	0	175	1.00	-0.30
10	51	88	45	0	184	1.13	-0.17
11	262	20	14	0	296	18.71	17.41
12	23	60	53	0	136	0.43	-0.87
13	23	50	21	0	94	1.10	-0.20
14	51	14	10	0	75	5.10	3.80
15	20	68	45	0	133	0.44	-0.86
16	24	132	60	0	216	0.40	-0.90
17	6	34	17	0	57	0.35	-0.95
18	19	71	30	0	120	0.63	-0.67
19	51	109	53	0	213	0.96	-0.34
20	53	38	41	0	132	1.29	-0.01
21	125	85	37	0	247	3.38	2.08
22	28	44	20	0	92	1.40	0.10
23	17	12	7	0	36	2.43	1.13
24	26	73	15	0	114	1.73	0.43
25	63	103	18	0	184	3.50	2.20
26	25	43	6	0	74	4.17	2.87
27	23	41	7	0	71	3.29	1.99
28	3	11	15	0	29	0.20	-1.10
29	13	46	39	0	98	0.33	-0.97
30	31	12	14	0	57	2.21	0.91
31	41	43	33	0	117	1.24	-0.06
32	67	113	89	0	269	0.76	-0.54
33	17	57	36	0	110	0.47	-0.83
34	19	99	77	0	195	0.24	-1.06
35	95	338	104	0	537	0.92	-0.38
36	115	24	15	3	157	7.67	6.37
37	29	72	47	0	148	0.62	-0.68
38	206	113	46	5	370	4.53	3.23
39	80	104	55	0	239	1.44	0.14
40	334	316	178	0	828	1.88	0.58
41	94	154	67	7	322	1.39	0.09
42	192	280	166	0	637	1.16	-0.14
43	21	74	50	1	146	0.42	-0.88
44	10	14	24	0	48	0.42	-0.88
45	20	28	32	0	80	0.63	-0.68
46	51	149	85	0	285	0.60	-0.70
47	71	32	22	0	125	3.23	1.93
48	22	63	39	0	124	0.56	-0.74

Tab. 5: Mafic mineral content in samples from present soil in plateau position as located in figure 4.
The amount of grains corresponds to 1 g of material from soil in the grain size range 105-420 µm. The ratio "clinopyroxene/titanite" was calculated for each sample in order to depict excesses of clinopyroxenes that should come from the Goldberg volcano. The excesses were obtained by discounting the ULST ratio (R=1.3) from the present soil ratios.
Tab. 5 : Contenu en minéraux mafiques d'échantillons prélevés dans le sol actuel sur des plateaux et localisés sur la figure 4. La quantité de grains correspond à 1 g de la fraction 105-420 µm extraite des échantillons de sol brut. Le rapport "clinopyroxène/titanite" a été calculé pour chaque échantillon de façon à mettre en exergue les excès de clinopyroxènes qui devraient provenir du volcan Goldberg. La valeur des excès a été obtenue en décomptant des rapports correspondants des échantillons du sol actuel, celui du ULST (R = 1,3).

– 33 samples display excesses E < 1. These values can be explained by quantitative variations within the ULST as demonstrated for the 1980 Mont St Helens tephra (Juvigné & Shipley, 1983).

– 9 samples display excesses within the range 1 < E < 6, and 6 samples are really clinopyroxene rich with

values E ≥ 6 up to E=17.4. Hence, at least the latter group possibly contains clinopyroxenes from other volcanoes and peculiarly from the Goldberg.

In addition, olivine is observed in four samples (tab. 5), to the east and south of the volcano (circled numbers in fig. 4). It has been shown that well preserved olivine crystals are lacking in the Goldberg surrounding tephra deposits, because the Goldberg olivine is highly broken and was destroyed by the explosive processes. Then, the olivine bearing sites must have been supplied by another Eifel volcano.

The geographical distribution of the ratios is represented in figure 4. Most of the samples displaying high excesses are in a westward position from the volcano. Since the other volcanoes of the WEVF are located at the SE of the Goldberg (the closest ones, 5 km away: Schönfelder Maar and Dehner Maar), and those of the EEVF at the East, this should imply that the pyroxenes (ULST excluded) high excesses should be expected on both side of the Goldberg. By the way, the current distribution should indicate that prevailing winds have spread the Goldberg tephra towards Belgium.

6.3 - DISCRIMINATION OF PYROXENES OF THE GOLDBERG TEPHRA AND OF THE ULST, IN SURROUNDING SOILS

Since it seems that the ULST and the Goldberg tephra possibly coexist at least in 6 sites (E ≥ 6), it was decided to go forward in the mineral determination in analyzing the pyroxenes from two sites that display respectively a large (#1: E = 7.4) and a very large (#11: E = 17.4) excess of clinopyroxenes, suggesting a major contribution of the Goldberg (tab. 6A).

For the pyroxenes of the ULST, we retain two analyses of Wörner & Schmincke (1984) from the LS site, and a set of analyses of Juvigné (1991) from the LS site and from four peatbogs in Germany and Belgium (tab. 6B).

	Soil #1				Soil #11			
An. #	62	61	65	71	84	77	78	79
SiO_2	44.42	46.01	48.22	50.40	44.42	46.02	48.58	51.52
TiO_2	3.34	2.28	1.99	0.99	3.62	2.14	1.77	0.91
Al_2O_3	7.23	7.56	4.42	4.21	7.87	7.11	4.76	3.96
FeO	8.10	8.54	5.46	4.59	7.09	8.43	4.90	4.15
MnO	0.10	0.24	0.11	0.00	0.15	0.17	0.01	0.05
MgO	12.01	11.03	14.17	15.11	12.24	11.35	14.21	15.74
CaO	24.19	23.28	24.23	23.69	24.13	23.13	24.01	22.87
Na_2O	0.26	0.86	0.22	0.41	0.18	0.81	0.25	0.44
K_2O	0.00	0.03	0.00	0.05	0.01	0.00	0.04	0.01
Cr_2O_3	0.03	0.00	0.19	0.06	0.12	0.08	0.64	0.37
Total	99.67	99.83	99.01	99.50	99.81	99.24	99.16	100.02
Si	1.666	1.719	1.798	1.854	1.661	1.728	1.806	1.882
Ti	0.094	0.064	0.056	0.027	0.102	0.061	0.050	0.025
Al	0.320	0.333	0.194	0.182	0.347	0.315	0.209	0.171
Fe^{3+}	0.175	0.163	0.106	0.084	0.137	0.163	0.080	0.036
Fe^{2+}	0.079	0.103	0.064	0.057	0.085	0.102	0.072	0.091
Cr	0.001	0.000	0.006	0.002	0.004	0.002	0.019	0.011
Mn	0.003	0.008	0.003	0.000	0.005	0.005	0.000	0.001
Mg	0.672	0.614	0.788	0.828	0.682	0.635	0.788	0.857
Ca	0.972	0.932	0.969	0.934	0.966	0.931	0.957	0.895
Na	0.019	0.062	0.016	0.029	0.013	0.059	0.018	0.031
K	0.000	0.002	0.000	0.002	0.000	0.000	0.002	0.000
Total	4.001	4.001	4.000	4.000	4.001	4.001	4.000	4.000
$100Mg/(Mg+Fe^{2+})$	89.53	85.59	92.50	93.61	88.97	86.21	91.60	90.45
Mg %	38.93	37.06	43.21	45.54	39.25	37.98	43.34	46.48
Fe" + Mn %	4.74	6.71	3.69	3.11	5.13	6.40	3.99	4.99
Ca %	56.33	56.23	53.10	51.34	55.62	55.62	52.66	48.53
End-members								
En %	33.59	30.73	39.51	41.49	34.16	31.79	39.78	43.09
Fs %	4.09	5.56	3.37	2.83	4.47	5.35	3.67	4.63
Wo %	36.75	35.77	41.56	40.82	36.72	36.17	41.93	40.84
Ac %	1.87	6.23	1.57	2.94	1.29	5.90	1.81	3.13
Jd %	0.00	0.00	0.00	0.00	0.00	0.00	0.00	0.00
Ca-Tsch %	0.00	5.21	0.00	3.64	0.75	4.30	1.52	5.27
Ti-Tsch %	8.02	6.40	4.90	2.75	10.19	6.05	5.00	2.52
Es %	15.67	10.10	9.09	5.52	12.43	10.42	6.29	0.53
Ko%	0.00	0.00	0.00	0.00	0.00	0.00	0.00	0.00
Total	100.00	100.00	100.00	100.00	100.00	100.00	100.00	100.00

Tab. 6A: Representative analyses of pyroxenes from the present soil samples. Table of detailed analyses can be obtained on request.
Tab. 6A : Analyses représentatives de pyroxènes provenant d'échantillons du sol actuel. Le tableau détaillé des analyses peut être obtenu sur demande.

	Laacher See area		Hinkelsmaar		Brackvenn		Konnerzvenn		Vance	
An. #	LS8	LS3	H1	H2	B5	B2	K5	K1	V1	V4
SiO_2	48.54	49.14	41.89	44.01	46.12	47.95	46.67	47.27	45.09	46.82
TiO_2	1.41	1.01	3.86	3.18	2.09	0.84	1.43	1.67	2.51	1.65
Al_2O_3	4.82	4.23	11.18	9.58	7.11	4.23	6.03	5.96	7.74	6.11
FeO	9.73	12.27	9.80	7.39	9.59	12.99	10.83	9.16	10.32	9.95
MnO	0.71	1.50	0.28	0.08	0.48	1.75	0.72	0.59	0.59	0.63
MgO	10.63	8.49	8.45	10.83	9.68	7.70	9.13	10.68	9.13	9.81
CaO	21.73	20.71	22.07	22.54	22.02	20.60	21.72	22.04	21.68	21.65
Na_2O	1.36	1.80	0.98	0.64	1.23	2.01	1.35	1.09	1.13	1.25
K_2O	0.00	0.01	0.01	0.01	0.01	0.03	0.01	0.02	0.01	0.00
Total	98.93	99.16	98.52	98.26	98.33	98.10	97.89	98.48	98.20	97.87
Si	1.836	1.876	1.603	1.669	1.759	1.855	1.795	1.794	1.730	1.795
Ti	0.040	0.029	0.111	0.091	0.060	0.024	0.041	0.048	0.072	0.048
Al	0.215	0.190	0.504	0.428	0.320	0.193	0.273	0.267	0.350	0.276
Fe^{3+}	0.132	0.131	0.140	0.100	0.134	0.197	0.154	0.130	0.129	0.131
Fe^{2+}	0.175	0.260	0.173	0.135	0.172	0.223	0.194	0.161	0.202	0.188
Mn	0.023	0.049	0.009	0.003	0.016	0.057	0.023	0.019	0.019	0.020
Mg	0.599	0.483	0.482	0.612	0.550	0.444	0.523	0.604	0.522	0.561
Ca	0.880	0.847	0.905	0.916	0.900	0.854	0.895	0.896	0.891	0.889
Na	0.100	0.133	0.073	0.047	0.091	0.151	0.101	0.080	0.084	0.093
K	0.000	0.000	0.000	0.000	0.000	0.001	0.000	0.001	0.000	0.000
Total	4.000	4.000	4.001	4.000	4.001	4.001	4.001	4.000	4.000	4.000
$100Mg/(Mg+Fe^{2+})$	77.37	65.00	73.55	81.96	76.21	66.57	72.96	78.93	72.10	74.92
Mg %	35.72	29.48	30.72	36.76	33.61	28.14	32.00	35.95	31.94	33.81
Fe^{2+} + Mn %	11.80	18.83	11.62	8.24	11.44	17.76	13.29	10.72	13.54	12.55
Ca %	52.48	51.69	57.66	54.99	54.95	54.10	54.71	53.32	54.52	53.63
End-members										
En %	29.96	24.17	24.10	30.62	27.51	22.21	26.17	30.23	26.11	28.02
Fs %	9.90	15.44	9.12	6.87	9.37	14.02	10.87	9.02	11.06	10.41
Wo %	37.85	37.66	30.96	33.78	35.93	36.75	36.60	36.93	34.69	36.62
Ac %	9.97	13.15	7.27	4.71	9.09	15.08	10.07	8.02	8.41	9.29
Jd %	0.00	0.18	0.00	0.00	0.00	0.00	0.00	0.00	0.00	0.00
Ca-Tsch %	5.04	6.50	10.69	9.71	7.81	4.84	6.81	6.10	7.98	7.08
Ti-Tsch %	4.01	2.90	11.11	9.07	5.99	2.45	4.14	4.77	7.24	4.76
Es %	3.27	0.00	6.76	5.25	4.29	4.64	5.35	4.93	4.51	3.82
Ko%	0.00	0.00	0.00	0.00	0.00	0.00	0.00	0.00	0.00	0.00
Total	100.00	100.00	100.00	100.00	100.00	100.00	100.00	100.00	100.00	100.00

Tab. 6B: Chemical composition of representative clinopyroxenes of the ULST.
Data for Laacher See area (LS8, LS3) are from Wörner & Schmincke (1984). Hinkelsmaar (H2, H1), Bragphenn (B2, B5), Konnerzvenn (K1, K5) and Vance (V4, V1) are three sites where the ULST is present in peat-bogs; their mafic minerals were analysed by Juvigné (1991). Table of detailed analyses (n = 30) can be obtained on request.
Tab. 6B : Composition chimique de pyroxènes représentatifs du ULST. Les valeurs pour les pyroxènes de la région du Laacher See (LS8, LS3) sont de Wörner & Schmincke (1984). Hinkelsmaar (H2, H1), Bragphenn (B2, B5), Konnerzvenn (K1, K5) et Vance (V4, V1) sont des sites où l'ULST est présent dans des tourbières ; les minéraux mafiques en ont été analysés par Juvigné (1991). Le tableau détaillé des analyses peut être obtenu sur demande.

The pyroxene analyses are plotted in the common Mg-Ca-Fe^{2+}+Mn diagram (fig. 7).

The pyroxenes of the soil sites # 1 and # 11 display the range composition of 46.4 < XMg % < 35.3, 8.9 < XFe^{2+}+Mn % < 1.7, 58.6 < XCa % < 48.3. Most of them plot in the area of the Goldberg volcano pyroxenes. A few pyroxenes, slightly richer in Fe and Na, can be related to the ULST. However, the contribution of another basaltic to nephelinitic West Eifel volcano cannot be excluded. The ULST pyroxenes are fassaitic diopside with the range composition of 36.8 < XMg % < 28.1,17.8 < XFe^{2+}+Mn % < 8.2, 58.1 < XCa % < 51.5. The fassaitic composition is due to their high Al and Na contents, and so, their high amount of Ca-tschermakite and acmite end-members. Compared to the Goldberg pyroxenes, the ULST pyroxenes are clearly more ferrous, and also richer in Al^{VI} and Na, in agreement with their phonolitic origin. Consequently, it is possible to discriminate the pyroxenes of the Goldberg tephra and those of the ULST.

The best discrimination is obtained in the diagram 100 $Mg/Mg+Fe^{2+}$ vs $Na+Al^{VI}$ (fig. 8). The Goldberg pyroxenes (volcano and most of the soil data) are richer in magnesia and poorer in Na and Al^{VI} than the ULST pyroxenes. This distinction is normal for mafic magma pyroxenes compared to evolved phonolitic magma pyroxenes.

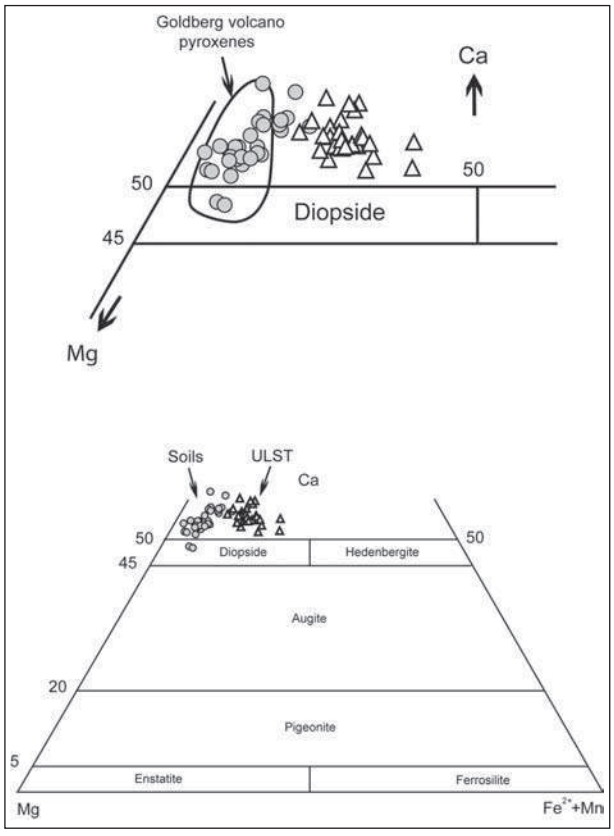

Fig. 7: Mg-Ca-Fe^{2+}+Mn diagram. Composition of pyroxenes from soil samples #1 and #11 (spots) and from the ULST (triangles) after Morimoto's classification (1998); comparison with the pyroxenes of the Goldberg volcano (delimited area).
Fig. 7 : Diagramme Mg-Ca-Fe^{2+}+Mn. Composition des pyroxènes des échantillons de sol #1 et #11 (pastilles), et ceux du ULST (triangles) d'après la nomenclature de Morimoto (1998) ; comparaison avec les pyroxènes du volcan Goldberg (zone encerclée).

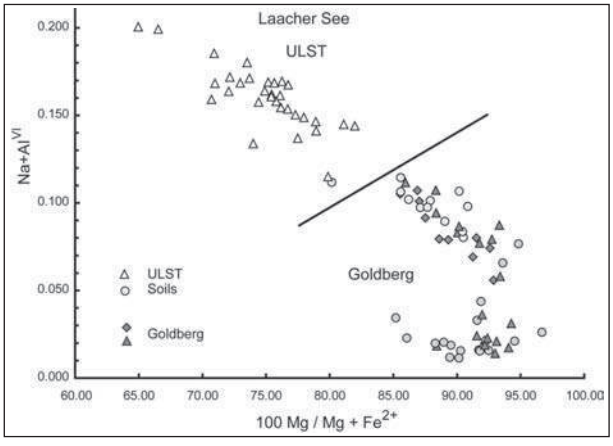

Fig. 8: 100 $Mg/Mg+Fe^{2+}$ vs $Na+Al^{VI}$ discrimination diagram for pyroxenes. Same symbols as for figures 5 and 8.
Fig. 8 : Diagramme de discrimination 100 $Mg/Mg+Fe^{2+}$ vs $Na+Al^{VI}$ pour les pyroxènes. Les symboles sont identiques à ceux des figures 5 et 8.

7 - ABOUT THE AGE OF THE GOLDBERG ERUPTION

Based on comparisons with a few dated volcanoes of the EWVF, Mertes (1983) and Mertes & Schmincke (1983) have used four criteria to estimate the age of non dated volcanoes in the same field. The Goldberg was placed in the group of volcanoes, which have erupted between 100 ka and 400 ka.

Magma composition. The magma of Goldberg is a leucite-nephelinite. A few K/Ar and $^{40}Ar/^{39}Ar$ ages of other volcanoes attest that leucitite-nephelinite have erupted in the WEVF throughout the Middle and the Late Pleistocene. This implies a time range from 780 ka to 11.6 ka.

Degree of morphological preservation for strombolian cones. The Goldberg is not a strombolian cone; hence this criterion cannot be applied.

Age relationship between volcanoes. The Goldberg is a solitary volcano at the NW margin of the WEVF (see above). The two closest ones (Schönfelder Maar and Dehner Maar) are located 5 km away from the Goldberg. They display similar composition, but they have not been either dated.

Relationship of the volcanoes and their products with river fluvial terraces. There is no terrace model for the river flowing around the Goldberg; hence this criterion cannot be applied.

As a conclusion, no evidence supports the integration of the Goldberg in a group of volcanoes that have erupted between 100 ka and 400 ka.

After our results, the following criteria can be added.

Minimal age after Bragphenn core. The Bragphenn is so close of the volcano (2 km), that Goldberg tephra should have been deposited on this site. But the Goldberg material is absent throughout the core so that the eruption is obviously older than the Upper Weichselian, i.e. older than 25 ka.

Removal of Goldberg tephra from proximal sites. At the time of the eruption, the plateaus surrounding the volcano should have been blanketed by a multi centimetre thick tephra layer, of which only traces remains in soils as shown by our analyses. This implies a long lasting erosion phase that predates the Upper Weichselian loess deposition (see Bragphenn).

Present soil development. The upper volcanoclastic beds of the Goldberg display a ghostly facies up to 2 m below the current surface. That deep alteration should likely involve not only the Holocene pedogenesis, but perhaps more ancient ones such as the interglacial Eemian one.

8 - CONCLUSION

The volcanological activity of the Goldberg volcano is somewhat clarified. Two important explosive events have been displayed. Then, at least regional deposition of tephra material may be assumed. In present soil samples in plateau position, the mafic minerals of the Laacher See Tephra are widely dominant. Nevertheless, based on geochemical analyses, the presence of clinopyroxenes from the Goldberg volcano is demonstrated in some samples indicating a westward spreading direction

from the volcano, i.e. towards Belgium. The long term erosion period that has followed the deposition of the Goldberg tephra explains the scattered occurrence of its minerals even in proximal sites. The minimal age of the eruption can be shifted from 11.6 ka BP to at least 25 ka BP.

ACKNOWLEDGMENT

The microprobe analyses were performed at the CAMST Centre of the University of Louvain-la-Neuve/ Belgium with the assistance of the Ing. Jacques Wautier, who is greatly acknowledged.

REFERENCES

BASTIN B., & JUVIGNÉ E., 1978 - L'âge des dépôts de la vallée morte des Chôdires (Malmedy). *Annales de la Société Géologique de Belgique*, **101**, 289-304.

BLOCKLEY S.P.E., BRONK RAMSEY C., LANE C.S., & LOTTER A.F., 2008 - Improved age modelling approaches as exemplified by the revised chronology for the Central European varved lake Soppensee. *Quaternary Science Reviews*, **27** (1/2), 61-71.

BRAUER A., ENDRES C., & NEGENDANK J.F.W., 1999a - Lateglacial calendar year chronology based on annually laminated sediments from Lake Meerfelder Maar, Germany. *Quaternary International*, **61** (1), 17-25.

BRAUER A., ENDRES C., GUNTER C., LITT T., STEBICH M., & NEGENDANK J.F.W., 1999b - High resolution sediment and vegetation responses to Younger Dryas climate change in varved lake sediments from Meerfelder Maar, Germany. *Quaternary Science Reviews*, **18** (3), 321-329.

BÜCHEL G., & LORENZ V., 1982 - Zum Alter des Maarvulkanismus der Westeifel. *Neues Jahrbuch für Geologie und Paläontologie Abhandlungen*, **163**, 1-22.

BUSTAMANTE SANTA-CRUZ L., 1974 - Pétrographie sédimentaire. Découverte d'une éruption du volcan d'Ormont. *Annales de la Société Géologique de Belgique*, **97**, 317-320.

COOLS S., 2004 - *Le Goldberg et la dispersion de sa cendre en direction de la Belgique*. Mémoire de Licence, Université de Liège, Département de Géographie, 119 p.

DAVIES S.M., HOEK W.Z., BOHNCKE S.J.P., LOWE J.J., O'DONNELL S.P., & TURNEY C.S.M., 2005 - Detection of Late-glacial distal tephra layers in the Netherlands. *Boreas*, **34** (2), 123-135.

FRECHEN M., 1999 - Upper Pleistocene loess stratigraphy in Southern Germany. *Quaternary Science Reviews*, **18** (2), 243-269.

FRECHEN M., OCHES E., & KOHFELD K., 2003 - Loess in Europe – mass accumulation rates during the Last Glacial Period. *Quaternary Science Reviews*, **22** (18/19), 1835-1857.

GEWELT M., & JUVIGNÉ E., 1986 - Les "téphra de Remouchamps", un nouveau marqueur stratigraphique dans le Pléistocène supérieur daté par $^{230}Th/^{234}U$. *Annales de la Société Géologique de Belgique*, **109**, 489-497.

GULLENTOPS F., 1954 - Contribution à la chronologie du Pléistocène et des formes du relief en Belgique. *Mémoires de l'Institut Géologique de l'Université de Louvain*, **18**, 125-252.

JUVIGNÉ E., 1977a - La zone de dispersion des poussières émises par une des dernières éruptions du volcan du Laacher See (Eifel). *Zeitschrift für Geomorphologie*, **21**, 323-342.

JUVIGNÉ E., 1977b - Zone de dispersion et âge des poussières volcaniques du tuf de Rocourt. *Annales de la Société Géologique de Belgique*, **100**, 13-22.

JUVIGNÉ E., & SEMMEL A., 1981 - Un tuf volcanique semblable à l'Eltviller Tuff dans les loess de Hesbaye (Belgique) et du Limbourg néerlandais. *Eiszeitalter und Gegenwart*, **31**, 83-90.

JUVIGNÉ E., & SHIPLEY S., 1983 - Distribution of the heavy minerals in the downwind lobe of the May 18, 1980 eruption of the Mount St Helens (Washington, U.S.A.). *Eiszeitalter und Gegenwart*, **33**, 1-7.

JUVIGNÉ E., & WINTLE A.G., 1988 - A new chronostratigraphy of the Late Weischelian loess units in Middle Europe based on thermoluminescence dating. *Eiszeitalter und Gegenwart*, **38**, 94-105.

JUVIGNÉ E., 1991 - Distribution de vastes retombées volcaniques originaires de l'Eifel et du Massif central aux temps post-glaciaires dans le N-E de la France et les régions voisines. *Comptes Rendus de l'Académie des Sciences de Paris, Série II*, **312**, 415-420.

JUVIGNÉ E., 1993 - Contribution à la téphrostratigraphie du Quaternaire et son application à la géomorphologie. *Mémoires pour servir à l'Explication des Cartes géologiques et minières de la Belgique*, **36**, 1-66.

MERTES H., 1983 - Aufbau und genese des Westeifeler Vulkanfeldes. *Bochumer Geologische und Geotechnische Arbeiten*, **9**, 1-415.

MERTES H., & SCHMINCKE H.-U., 1983 - Age distribution of volcanoes in the West Eifel. *Neues Jahrbuch für Geologie und Paläontologie Abhandlungen*, **166**, 260-283.

MORIMOTO N., 1988 - Nomenclature of pyroxenes. *Bulletin de Minéralogie*, **111** (5), 535-550.

POUCLET A., JUVIGNÉ E., & PIRSON S., 2008 - The Rocourt Tephra, a widespread 90-74 ka stratigraphic marker in Belgium. *Quaternary Research*, **70** (1), 105-120.

POUCLET A., & JUVIGNÉ E., 2009 - The Eltville tephra, a late Pleistocene widespread tephra layer in Germany, Belgium and The Netherlands; symptomatic compositions of the minerals. *Geologica Belgica*, **12** (1/2), 93-103.

PREUSSER F., & FRECHEN M., 1999 - Chronostratigraphie der oberweichselzeitlichen Loessabfolge von Ockenfels (Mittelrhein). *In* R. Becker-Haumann & M. Frechen (ed.), *Terrestriche Quartärgeologie*. Logabook, Köln, 68-80.

RAHM G., 1961 - Der Goldberg bei Ormont und der Kreuzberg bei Schoenbach, zwei bemerkenswerte Tuffvulkane des Westeifel. *Decheniana*, **1961**, 53-60.

REIMER P.J., BAILLE M.G.L., BARD E., BAYLISS A., WARREN B.J., CHANDA B.J.H., BLACKWELL P.G., BUCK C.E., BURR G.S., CUTLER K.B., DAMON P.E., EDWARDS R.L., FAIRBANKS R.G., FRIEDRICH M., GUILDERSON T.P., HOGG A.G., HUGHEN K.A., KROMER B., MCCORMAC G., MANNING S., BRONK RAMSEY C., REIMER R.W., REMMELE S., SOUTHON J.R., STUIVER M., TALAMO S., TAYLOR F.W., VAN DER PLICHT J., & WEYHENMEYER C.E., 2004 - IntCal04 terrestrial radiocarbon age calibration, 0-26 cal kyr BP. *Radiocarbon*, **46** (3), 1029-1058.

ROHDENBURG H., & SEMMEL A., 1971 - Bemerkungen zur stratigraphie des Würm-Lösses im westlichen Mitteleuropa. *Notizblatt des Hessischen Landesamtes für Bodenforschung zu Wiesbaden*, **99**, 246-252.

STRAKA H., 1975 - Die Spätquartären Vegetationsgeschichte der Vulkaneifel. *Beiträge zur Landespflege in Rheinland-Pfalz*, **3**, 1-163.

VAN DEN BOGAARD P., 1995 - $^{40}Ar/^{39}Ar$ ages of sanidine phenocrysts from Laacher See Tephra (12,900 yr BP): Chronostratigraphic and petrological significance. *Earth and Planetary Science Letters*, **133** (1/2), 163-174.

VAN DEN BOGAARD P., & SCHMINCKE H.-U., 1985 - Laacher See tephra: a widespread isochronous late Quaternary Tephra layer in central and northern Europe. *Geological Society of America Bulletin*, **96** (12), 1554-1571.

WOILLARD G., 1975 - Recherches palynologiques sur le Pléistocène dans l'Est de la Belgique et dans les Vosges lorraines. *Acta Geographica Lovaniensia*, **14**, 1-118.

WÖRNER G., & SCHMINCKE H.-U., 1984 - Mineralogical and chemical zonation of the Laacher See Tephra sequence (East Eifel, W. Germany). *Journal of Petrology*, **25** (4), 805-835.